

# Chapter 4

## Blank Materials



Eren Billur and Hyun-Sung Son

**Abstract** All sheet metal forming operations start with the blank material. The final part properties are dependent on the incoming material properties and how they could be changed during the process. To engineer the final part, it is essential to understand the incoming blank material. This chapter discusses the most common 22MnB5 steel, and other steel grades already in use or proposed to be used in hot stamping processes. Incoming blank could be uncoated or coated. Coatings can affect the final properties due to scale formation, decarburization and by the presence of microcracks. In the last decade, tailored blanks have been used in a number of automotive applications. The last section of this chapter summarizes Tailor Rolled, Patchwork, Tailor Welded blanks, and their combinations.

### 4.1 22MnB5

Currently, most of the production and research is being done using 22MnB5 grade (Material number 1.5528). This is a low-carbon steel, with manganese and boron alloying. The chemical composition of 22MnB5 is given in Table 4.1. As delivered, the steel has a yield strength of approximately 400 MPa, UTS around 600 MPa and approximately 22% total elongation. After quenching, the material's yield strength exceeds 1000 MPa and UTS reaches 1500 MPa. The total elongation of the final part is typically over 5% [1–3] (Fig. 4.1).

---

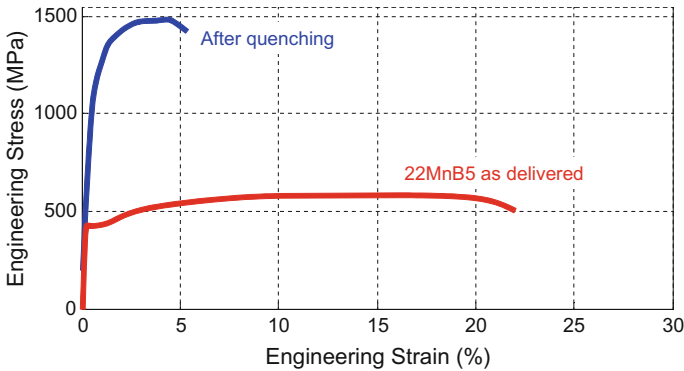
E. Billur (✉)  
Billur Makine Ltd., Ankara, Turkey  
e-mail: eren@billur.com.tr

E. Billur  
Atılım University, Ankara, Turkey

H.-S. Son  
POSCO Global R&D Center, Incheon, South Korea  
e-mail: hsson@posco.com

**Table 4.1** Chemical composition of 22MnB5 [4–6]

	C	Mn	B	Cr	Si	Al	Ti	N
Minimum	0.19	1.10	0.0008	0.10	0.00	0.02	0.015	0.000
Nominal	0.22	1.18	0.0020	0.16	0.22	0.03	0.040	0.005
Maximum	0.25	1.40	0.0050	0.35	0.40	0.08	0.050	0.010

**Fig. 4.1** Engineering stress–strain curves of 22MnB5, in as-delivered conditions and after quenching (re-created after [2])

This alloy has been commercialized by several names, including but not limited to:

- Ultralume by AK Steel, available as uncoated or Al/Si coated [7].
- USIBOR 1500 by ArcelorMittal, typically AlSi-coated steel produced and patented by ArcelorMittal. Zn-coated versions are also available by the name USIBOR 1500 GI or GA [8, 9].
- BR 1500 HS: by BaoSteel [10],
- BTR 165: uncoated steel by Benteler [11],
- SQ 1500: (Sumi-quenth) by Nippon-Sumitomo [12],
- Hot Press Forming (HPF) 1470 by posco, available uncoated, AlSi coated or Zn (GI) coated [13, 14]
- Docol 1500 PHS: uncoated steel by SSAB, earlier named as Docol 1500 Bor [15, 16]
- MBW1500: Mangan-Bor-Stahl zum Warmumformung, literally meaning manganese-boron steel for hot form hardening, produced by ThyssenKrupp. Available uncoated or AlSi coated (MBW1500+AS) [17]. There was a ZnNi-coated version [18] which was later discontinued [19, 20].
- phs-ultraform 1500: Zn-coated steel by voestalpine [21]
- WHT1500HF: uncoated steel by Wisco [22].<sup>1</sup>

<sup>1</sup>Steel companies are listed alphabetically.

## 4.2 Higher Strength Steels (>1700 MPa)

Mn-B alloyed steels have been long available in hot-rolled (i.e., thick blanks) and uncoated conditions for agriculture and construction machinery industries [23]. Chemical compositions of several standard Mn-B and Mn-B-Cr alloyed steels that have higher carbon than 22MnB5 are tabulated in Table 4.2 [1, 6].

Mn-B alloyed steels are typically delivered in soft, ferritic-pearlitic condition. First, they have to be austenitized in an atmosphere controlled furnace. Once quenched, their strength levels are at least doubled, as listed in Table 4.3. Steels with higher carbon level than the most common 22MnB5 typically have higher strength. These grades may save even more weight, with equivalent intrusion resistance [12, 24, 25]. For hot stamping applications, some of the steels listed in Tables 4.2 and 4.3 are slightly modified and commercialized under different names.

**Table 4.2** Chemical compositions (wt-%) of higher strength Mn-B and Mn-B-Cr steels (trace amounts of other elements, balance Fe) [1, 4, 6]

Steel	(Mat'l number)	C	Mn	B	Cr
27MnCrB5	(1.7182)	0.25	1.24	0.002	0.34
28MnB5		0.28	1.30	0.005	–
30MnB5	(1.5531)	0.30	1.30	0.005	–
33MnCrB5	(1.7185)	0.33	1.35	0.005	0.45
34MnB5		0.34	1.30	0.005	–
37MnB4	(1.5537)	0.33	0.81	0.001	0.19

**Table 4.3** Yield and Ultimate Tensile Strength of several quenchant steels before and after quenching [1, 4, 6]

Steel	As delivered		Quenched	
	Yield stress MPa (ksi)	UTS MPa (ksi)	Yield stress MPa (ksi)	UTS MPa (ksi)
27MnCrB5 (1.7182)	478 (69)	638 (93)	1097 (159)	1611 (234)
28MnB5	420 (61)	620 (90)	1135 (165)	1740 (252)
30MnB5 (1.5531)	510 (61)	700 (90)	1230 (165)	1740 (252)
33MnCrB5 (1.7185)	420 (61)	620 (90)	1290 (187)	1850 (268)
34MnB5	600 (87)	820 (119)	1225 (178)	1919 (278)
37MnB4 (1.5524)	580 (84)	810 (117)	1378 (200)	2040 (296)

For example, ArcelorMittal has been developing a steel grade similar to 34MnB5, commercially named as USIBOR® 2000P, which is currently under customer trials. This grade will be available with AlSi coating [8, 31]. Baosteel is also preparing a 1800 MPa steel [13].

Mazda has become the first vehicle manufacturer to use higher strength boron steels. The CX-5 (SOP 2011) has 1,800MPa (~260ksi) tensile strength reinforcements in front and rear bumpers, Fig. 4.3. According to Mazda, the new material saved 4.8 kg (~10.6lbs.) per vehicle. The material was supplied by Sumitomo Metals (SumiQuench 1800, SQ1800 as shown in Fig. 4.2, modified 30MnB5) and hot stamped at a facility of Aisin Takaoka, both in Japan [12, 32]. Figure 4.4 shows the comparison of bumper beams with SQ1500 and SQ1800. With the higher strength material, it was possible to save 12.5% weight with equal performance [12].

Posco has already demonstrated HPF 2000 steel in a number of component-based examples, and also in the Renault EOLAB concept car [28, 33]. Since 2016, Posco has also been developing a 1800MPa grade [14]. SSAB has already commercial-

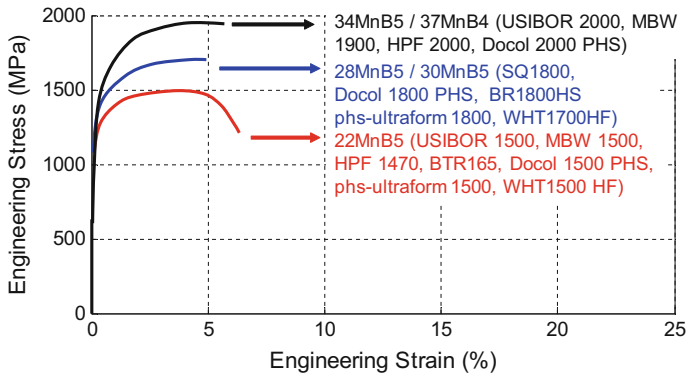


**Fig. 4.2** Engineering strain–stress diagram for 22MnB5 and higher strength boron steels (re-created after: [12, 24, 26–30]). Note that some of these grades may not be commercially available

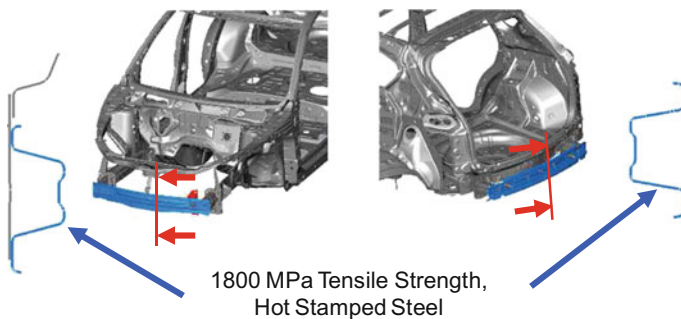


**Fig. 4.3** Bumper beam reinforcements of Mazda CX-5 (SOP 2011) are the first automotive applications of higher strength boron steels [32]

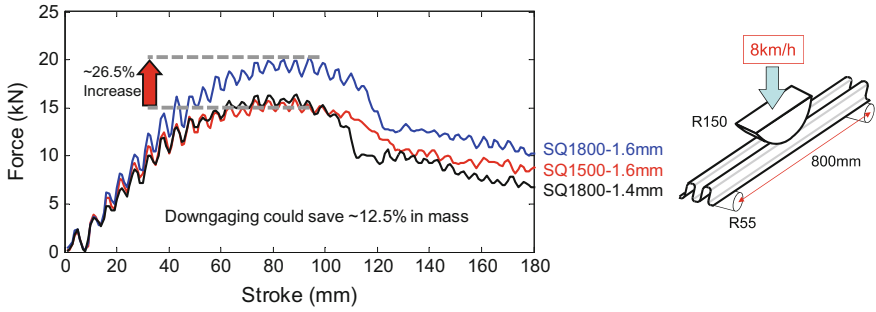


Fig. 4.4 Comparison of bumper beams with SQ1500 and SQ1800 (re-created after [12])

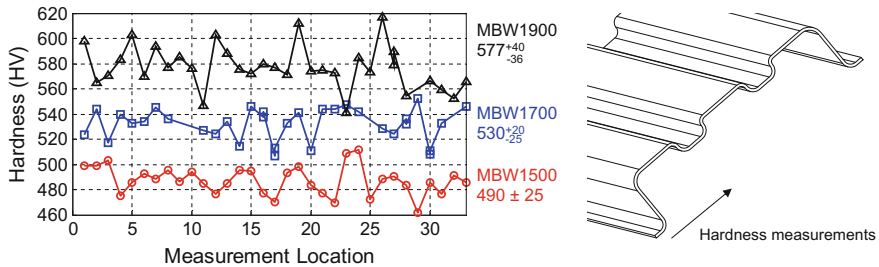


Fig. 4.5 Hardness distribution of an impact beam using ThyssenKrupp Mn-B steels (re-created after [18, 26])

ized uncoated Docol PHS 1800 (~30MnB5) and is preparing Docol PHS 2000 [34]. ThyssenKrupp has demonstrated that an MBW® 1900 B-pillar with correct properties can save 22% weight compared to DP600 and yet costs 9% less than the original dual-phase design [35]. Ford had also demonstrated that by using MBW 1900 instead of 22MnB5, a further 15% weight could be saved [24]. Another grade in development by ThyssenKrupp was MBW® 1700 (28MnB5). Figure 4.2 shows MBW® 1900 (34MnB5) tensile data, compared with MBW® 1700 (28MnB5) and MBW® 1500 (22MnB5), with commercial names from other suppliers as well [27]. Voestalpine has already commercialized phs-ultraform 2000 [36].

Table 4.4 summarizes commercially available and under development steel grades, designed for hot stamping applications.

Vickers Hardness (HV) values for conventional 22MnB5 steel are in the order of 450–500 HV after quenching. 37MnB4, on the other hand, has a Vickers Hardness of 600–610 HV [4]. Similarly, Overrath et al. [26] found ~490 HV for MBW® 1500, ~530 HV for MBW® 1700 and ~580 HV for MBW® 1900, as shown in Fig. 4.5. ThyssenKrupp has commercialized MBW® 1900 in 2013 [42]. MBW 1700 has not been commercialized yet [43].

Problems with higher strength materials are (1) their low toughness/energy absorption (i.e., typically even lower elongation than 22MnB5, see Fig. 4.2), (2) delayed

**Table 4.4** Chemical compositions, final properties, and commercial availability of >1700MPa steels specifically designed for hot stamping applications [12, 14, 27, 31, 34, 36-41]

Steel <sup>a</sup>	Chemical Composition (%wt)					Yield (MPa)	Tensile (MPa)	Elongation (%)	Bending Angle	Availability	
	C	Mn	B	Nb						U/C	AISI
USIBOR 2000	0.37	1.4	0.005	-		≥1400	≥1800	≥3	≥45°	-	+
BR1800 HS	-	-	-	-		≥1200	≤1800	≥5	-	-	-
SQ 1800	0.30	1.8	0.002	0.08		1267	1882	7.6	-	-	+
HPF 1800						≥1200	≥1750	≥6	-	*	+
HPF 2000						≥1300	≥1900	≥5.5	-	*	-
Docol 1800 PHS	0.27-0.33	1-1.35	≤0.005	-		1300	1800	6	-	+	-
Docol 2000 PHS	0.36-0.42	1.15-1.45	≤0.005	-		1700	2000	3.7	-	*	-
MBW 1700	0.26-0.30	1.15-1.45	≤0.005	-		~1150	≥1700	≥4	-	-	-
MBW 1900	0.32-0.38	1.0-1.4	≤0.005	-		≥1200	≥1900	≥4	55-65°	+	-
phs-ultraform 2000	0.20-0.36	≤2.0	≤0.005	≤0.01 (incl. Ti)		≥1100	≥1800	≥5	≥45°	-	+

\*Under development

<sup>a</sup>Steel companies are listed alphabetically

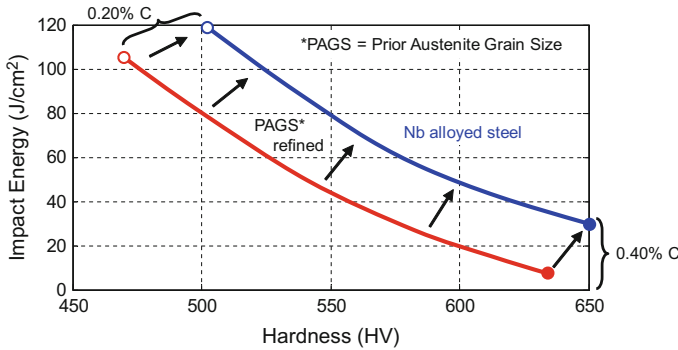


**Fig. 4.6** Energy absorbing capacity decreases with increased hardness. If “Prior Austenite Grain Size” (PAGS) can be refined, significant improvements can be achieved [re-created after [41, 42]]

cracking and (3) weldability [12]. Delayed cracking is investigated in Sect. 6.19 and weldability in Chap. 7.

Naderi [4] noted that, during tensile test of 37MnB4 (UTS = 2040 MPa, 296 ksi), all of the hardened tensile samples were cracked out of the gage length. One possible way to improve the toughness (energy absorbing capacity) of higher strength steels is grain refinement. Wang et al. had shown that as the “prior austenite grain size” (PAGS) of a high-strength steel is reduced, both the strength and elongation values are improved. Thus, the toughness is improved [44]. Figure 4.6 shows energy absorption of martensitic steels with hardness between 450–650 HV - in the range of most hot stamping grades. When Nb alloying is introduced, the toughness is increased through PAGS refinement [41].

### 4.3 Higher Elongation/Energy Absorbing Materials

Since hot-stamped parts are extremely strong, but do not absorb much energy, they are mostly used where intrusion resistance is required. However, lately, there are new materials for hot stamping which have higher elongation (ductility) compared to 22MnB5. Thus, these materials can save weight where energy absorption is required.

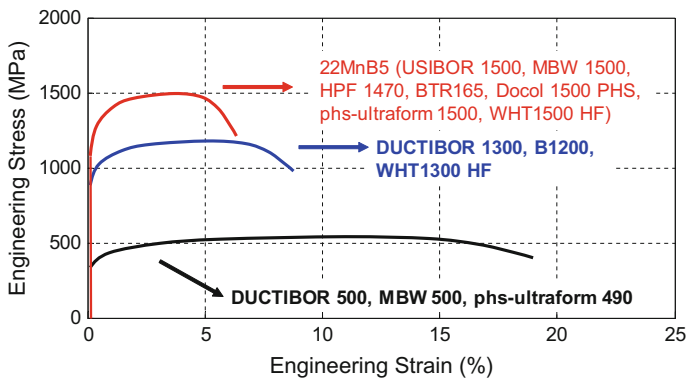
These new grades can be investigated in two different strength levels:

- (1) 450–600 MPa tensile strength level and >15% total elongation and
- (2) 1000–1300 MPa tensile strength level and >5% total elongation.

ArcelorMittal has been developing 4 new materials, as shown in Table 4.5. Figure 4.7 shows the approximate engineering strain–stress diagrams of USIBOR 1500 (22MnB5), DUCTIBOR 1300 and 500. There is also research going on laser welding DUCTIBOR grades to USIBOR grade material to combine intrusion resis-

**Table 4.5** Higher elongation hot stamping materials, developed by ArcelorMittal [8, 31, 47]

Product name	Yield strength MPa (ksi)	Tensile strength MPa (ksi)	Elongation (%)	Status
DUCTIBOR 450	340–460 (50–65)	460–610 (65–90)	≥16	Industrial
DUCTIBOR 500	370–470 (55–70)	550–700 (55–100)	≥16	Industrial
DUCTIBOR 1000	≥800 (≥115)	≥1000 (≥145)	≥6	Customer testing
DUCTIBOR 1300	≥950 (≥135)	≥1300 (≥190)	≥5	n/a

**Fig. 4.7** Comparison of 22MnB5 with high elongation grades [8, 10, 43, 49, 52]

tance and energy absorption properties. For details of these studies, see Sect. 8.2.1 [8, 45]. Since 2015, several Fiat models have a rear rail with Ductibor 450 [46].

ThyssenKrupp and voestalpine have also developed 500 MPa (~75 ksi) grades with the commercial names MBW® 500 and phs-ultraform 490, respectively. Production of MBW® 500 started in January 2012. Since 2014, Volvo is using MBW500 steel in the new XC90 in energy absorbing areas [48]. Since then, ThyssenKrupp also developed MBW® 600 [43], voestalpine rolled phs-ultraform 490, which is available with Zn coating, in February 2013 [49].

For crashworthiness, bending angle may be a more important indicator compared to total elongation [50]. Thus, bending angles are also reported in the summary of 450–600 MPa steels is given in Table 4.6.

In 1000–1300 MPa tensile strength grades, BaoSteel has commercialized B1200 steel since 2013. This steel has minimum 900 MPa yield, 1200 MPa tensile strength when quenched properly and can still have 7% uniform elongation [10]. WISCO has also commercially available 1300 MPa grade, WHT 1300 HF [22, 53]. As of 2017, Ductibor 1000 is under customer testing, and there are no updates about Ductibor 1300 [31] (Table 4.7).



**Table 4.6** Chemical compositions, final properties, and commercial availability of 450–600MPa steels [31, 43, 49, 51]

Steel <sup>a</sup>	Chemical Composition (%wt)				Yield (MPa)	Tensile (MPa)	Elongation (%)	Bending Angle	Availability		
	C	Mn	B	Si					U/C	AISI	Zn
Ductibor 450	≤0.11	≤1.1	≤0.001	≤0.06	≥350	≥460	≥16	≥120°	–	+	*
Ductibor 500	≤0.1	≤1.3	≤0.001	≤0.5	≥400	≥550	≥16	≥120°	–	+	–
MBW® 500	≤0.10	≤1.0	≤0.005	≤0.35	≥400	≥550	≥17	≥140°	–	+	–
MBW® 600	≤0.10	≤2.0	≤0.005	≤0.5	≥450	≥650	≥16	–	–	+	–
phs-ultraform 490	≤0.11	≤1.4	–	≤0.5	≥340	≥460	≥12	≥120°	–	–	+

<sup>a</sup>Steel companies are listed alphabetically

**Table 4.7** Chemical compositions, final properties and commercial availability of 1000–1300MPa steels [22, 31, 54, 55]

Steel <sup>a</sup>	Chemical Composition (%wt)			Yield (MPa)	Tensile (MPa)	Elongation (%)	Bending Angle	Availability		
	C	Mn	Si					U/C	AISI	Zn
Ductibor 1000	≤0.12	≤2.0	≤0.06	≥800	≥1000	≥6	≥80°	-	+	-
BR1200 HS	0.16-0.20	1.0-1.5	≤0.0030	≥900	≥1200	≥8	-	+	-	-
WHT1300 HF	0.2	1.15	≤0.005	≥950	≥1300	≥8	-	+	-	-

<sup>a</sup>Steel companies are listed alphabetically

## 4.4 Other Steels for Hot Stamping

In the last few years, new steels are also considered for hot stamping process. Although these are not in mass production yet, research and development were done on hot stamping of:

- (1) Stainless steels,
- (2) Medium-Mn steels (including steels with higher Mn content compared to 22MnB5),
- (3) Sandwich materials.

### 4.4.1 *Stainless Steels*

Aperam and Outokumpu have already demonstrated stainless steel grades that can be formed in the current hot stamping lines. Aperam's method is to get almost 100% martensitic structure, whereas Outokumpu recommends duplex (Austenite + Martensite) microstructure after hot forming and quenching [56, 57]. Stainless steels are corrosion resistant by their nature in service conditions. They also do not require a special coating or controlled atmosphere at hot conditions [58].

Aperam has already developed three different steels for hot stamping, one for intrusion resistance applications and two for energy absorbing areas. The chemical compositions and mechanical properties are tabulated in Table 4.8. According to Herbelin, almost 100% martensite can be formed at very low cooling rates (as low as 1 °C/s, as shown in Fig. 4.8), thus parts produced with this steel could be air hardened [58]. The low critical cooling rate allows the part to be formed in a multistep operation (Fig. 4.22) [59].

Outokumpu has shown that Nirosta 1200 PH grade can be hot formed, which would have 1100–1300 MPa yield and 1700–1850 MPa tensile strength, combined with 12–16% total elongation after quenching (see Table 4.8) [56]. The material can save weight both in intrusion resistance components and energy absorbing components, since it can absorb three times the energy 22MnB5 can absorb. Figure 4.9 shows the comparison of Nirosta 1200 PH and 22MnB5. This material is classified as duplex stainless steel, as it contains austenite and martensite.

### 4.4.2 *Medium-Mn Steels*

Medium-Mn steels are being developed both for cold and hot stamping applications. There are several advantages of medium-Mn steels over 22MnB5 in hot stamping:

(1) **Austenitization temperature is typically lower** than 22MnB5 and decreases with increasing Mn content. This could reduce the energy requirement of the furnaces and save energy and cost (see Fig. 4.11) [62, 63].

**Table 4.8** Chemical compositions and final properties (after hot stamping and quenching) of stainless steels designed for hot stamping [56–58, 60, 61]

Steel <sup>a</sup>	Chemical Composition (%wt)						Yield (MPa)	Tensile (MPa)	Elongation (%)	Bending Angle
	C	Mn	Cr	Ni	Others					
MaX 1.2	0.10	0.4	12	0	Nb	>800	~1200	>10	>65°	
MaX 1.2 HY	0.06	+	11	0.5	Nb	>800	~1200	~10	>95°	
MaX 2	0.2–0.25	>0.3	13	0–2	Nb	>1000	~1800	~10	–	
H1200 PH	0.43–0.5	<1.0	13.5±1	0	–	1100–1300	1700–1850	12–16	–	

<sup>a</sup>Steel companies are listed alphabetically

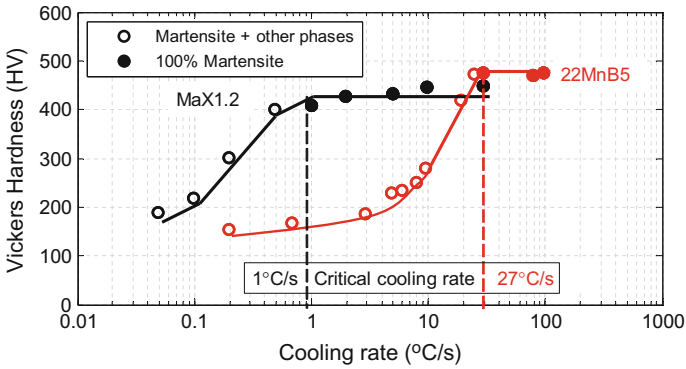


**Fig. 4.8** Critical cooling rate comparison of MaX 1.2 and 22MnB5 (re-created after: [58])

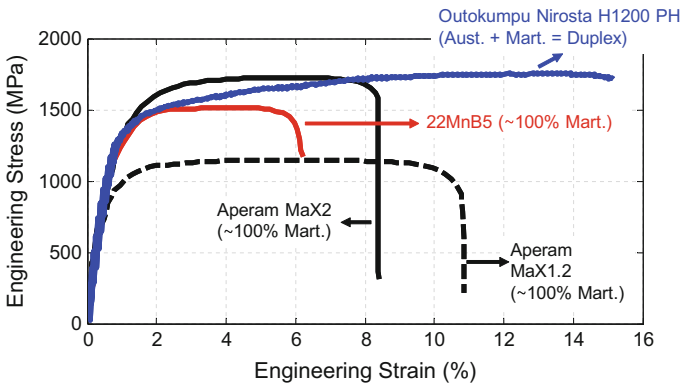


**Fig. 4.9** Comparison of 22MnB5 with potential new hot stamping stainless steel grades. All curves shown here are after hot stamping and quenching (re-created after: [56, 58])

**(2) Martensitic transformation can occur at very low cooling rates** and thus simple dies could be built for hot forming of these grades, as they could be air hardened. They can also be formed in multistep operations. Martensite start/finish temperatures are also lower than 22MnB5 [64, 65].

**(3) Some retained austenite may be present** in the final part. Medium-Mn steels, when properly hot stamped, may have high strength and high elongation. For example, tensile strength of 1800 MPa could be achieved with 10% total elongation, similar to the high yield strength medium-Mn steel shown in Fig. 4.10 [62]. Yi et al. achieved 1880 MPa tensile strength with 16% total elongation [66]. Rana et al. studied a number of heat treatment conditions with a 10 wt.% Mn steel and achieved 1330-1450 MPa tensile strength with 16–25% total elongation [67].

Recently, BaoSteel has shown two medium-Mn grades for hot stamping applications. One of these steels was designed for intrusion resistance applications and have high yield strength, in the order of 1000–1050 MPa (~145–150 ksi). As shown in

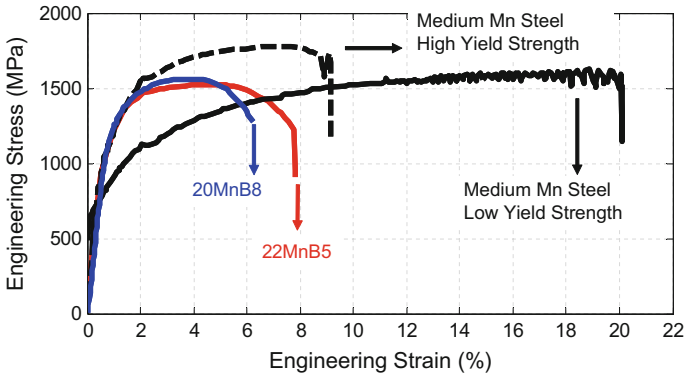


**Fig. 4.10** Engineering stress–strain curves of 20MnB8, 22MnB5, and medium-Mn steels (re-created after: [20, 30, 62])

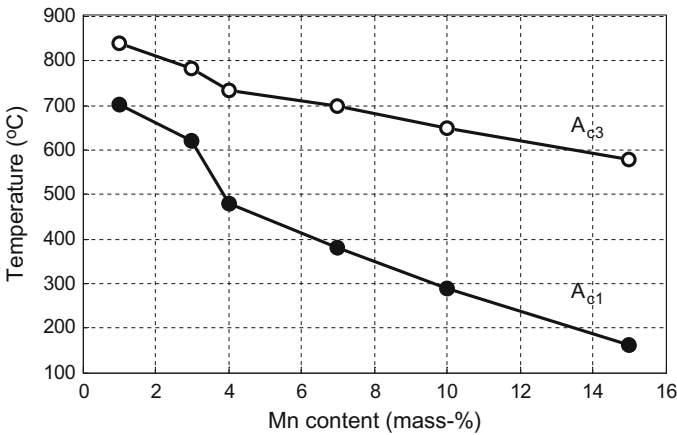


**Fig. 4.11** Effect of Mn content on equilibrium transformation temperatures (re-created after: [62])

Fig. 4.10, the low yield strength version has 20% total elongation and approximately 1500 MPa (215 ksi) tensile strength. The chemical compositions were not published yet, but the austenitization temperatures were listed as 750–850 °C (~1350–1600 °F) [30].

Han et al. have calculated the austenitization temperatures using ThermoCalc software [62]. As shown in Fig. 4.11, the furnace temperature can be reduced with increased Mn content. A study funded by the EU for energy efficient hot stamping has shown that a typical industrial furnace consumes 32 m<sup>3</sup>/h gas for mass production 22MnB5 at furnace temperature of 930 °C. When the furnace temperature was reduced to 808 °C the consumption went down to 19 m<sup>3</sup>/h and at 785 °C it was as low as 17 m<sup>3</sup>/h [63]. Thus, a medium-Mn steel may save energy in the life cycle assessment (Table 4.9).

**Table 4.9** Chemical compositions and final properties (after hot stamping and quenching) of medium-Mn steels designed for hot stamping [56–58, 60, 61]

Reference	Chemical Composition (%wt)				Yield (MPa)	Tensile (MPa)	Elongation (%)
	C	Mn	B	Others			
20MnB8 [68]	0.195	1.98	0.003	Ti, Cr,...	>1000	~1500	>8
BaoSteel [30] Low Yield Strength	n/a	n/a	n/a	n/a	690	1620	20.0
BaoSteel [30] High Yield Strength	n/a	n/a	n/a	n/a	1045	1770	9.2
BaoSteel [30] Medium-Mn [62]	0.1–0.2	5–12	0	Ti+V	>900	~1800	~10
Medium-Mn [64]	0.22	4–7	0.0024	Ti	1220	1519	>11.8

Manganese alloying reduces martensite start–finish temperatures ( $M_s$  and  $M_f$ ) and also retards bainite formation. For 20MnB8 (2.0%-wt. Mn), the critical cooling rate is around 20 °C/s (36 °F/s) [68]. In medium-Mn steels (4–7%-wt. Mn), even 10 °C/s (18 °F/s) could be sufficient for 100% martensitic transformation [64].

### 4.4.3 Steel Composites

ThyssenKrupp has been developing a family steel composites, called TriBond ®, since 2006 [69]. Here, three slabs (one core material and two cladding layers) are surface prepared, stacked on top of each other, and welded around the edges. Initially, TriBond ® was designed for wear-resistant cladding and ductile core materials [69].

In 2014, the original composite was modified for hot stamping. The core material was 22MnB5 and the thinner cladding layers were ductile material (MBW 1500 and MBW 500 respectively), as shown in Fig. 4.12. Coilmaking process was also slightly modified: after hot rolling, the slabs were then cold rolled, annealed, and aluminum coated [70]. As tabulated in Table 4.10, there are currently two planned versions of Tribond with approximately 1200 and 1400 MPa tensile strength (~175 and 205 ksi respectively). Both grades have higher bending angles compared with 22MnB5 after quenching [71].

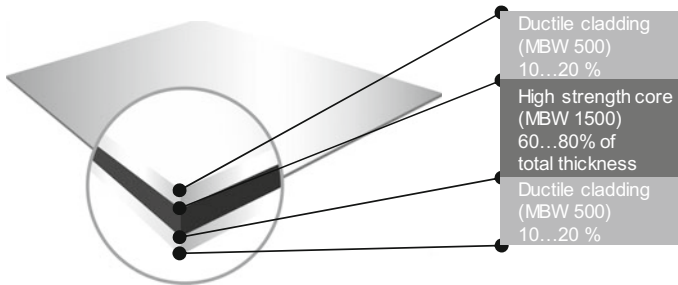


**Fig. 4.12** Schematic view of Tribond® grades (re-created after [72])

**Table 4.10** Through thickness compositions and final properties of ThyssenKrupp hot forming composites [17, 51, 71]

Steel	Through thickness composition	Yield (MPa)	Tensile (MPa)	Elongation (%)	Bending Angle
MBW 500+AS	100% MBW500	≥400	≥550	≥17	140–155°
MBW 1500+AS	100% MBW1500	≥1000	≥1400	>5	≥55°
TRIBOND®1200+AS	20% MBW500 60% MBW1500 20% MBW500	≥730	≥1100	>5	≥135°
TRIBOND®1400+AS	10% MBW500 80% MBW1500 10% MBW500	≥890	>1300	>5	≥75°



## 4.5 Coatings

As discussed in Chap. 3, uncoated boron steels suffer from scaling, which adds up another manufacturing step of descaling. Coating the blank does not only solve the scaling problem, but also improves protection against corrosion and reduces the risk of decarburization [21, 73].

If the steel's surface is not coated and exposed to high-temperature atmosphere, oxygen and other oxidizing gases react with the steel. Thus, scale forms on the surface—an oxide layer, typically composed of  $Fe_3O_4$  [74]. The scale must be cleaned by sandblasting after hot forming process [1].

Another phenomenon happening during high-temperature heating is “surface decarburization”. If the conditions are favorable for iron ( $Fe$ ) to oxidize, it may also be possible for carbon ( $C$ ) to be oxidized as well. If the carbon is oxidized to produce gaseous carbon monoxide and/or carbon dioxide ( $CO$  and/or  $CO_2$ ), a layer close to the surface would lose their carbon content [76]. As discussed in earlier sections, carbon is one of the most important alloying element affecting the final hardness. Choi and De Cooman studied the effects of decarburization of uncoated 22MnB5 steel. They found that the depth of decarburization layer increases with time, until the oxide layer forms a barrier between the steel and atmosphere. As the carbon is depleted in near-surface regions, the hardness is lowered (Fig. 4.13a) [50]. Decarburization is usually undesirable since it lowers the strength/hardness and may affect fatigue life [77]. However, in the case of 22MnB5, lower carbon layers close to the surface creates a composite with high-strength core and ductile layers, similar to the one explained in previous subsection. As a result, bendability may improve with decarburized layers, as shown in Fig. 4.13 [50].

Belanger [78] estimated that only 38% of hot stamped components in auto-body will be in dry areas. Therefore, high cathodic protection is required in 62% of hot-stamped components. Currently, most coated boron steels sold are AlSi coated, which only offer barrier corrosion protection. Zn-based coatings are favored for their cathodic protection, but may require indirect hot stamping followed by an additional surface cleaning process, such as sandblasting [79]. Table 4.11 is a summary of coatings available in the market and/or proposed for hot stamping.

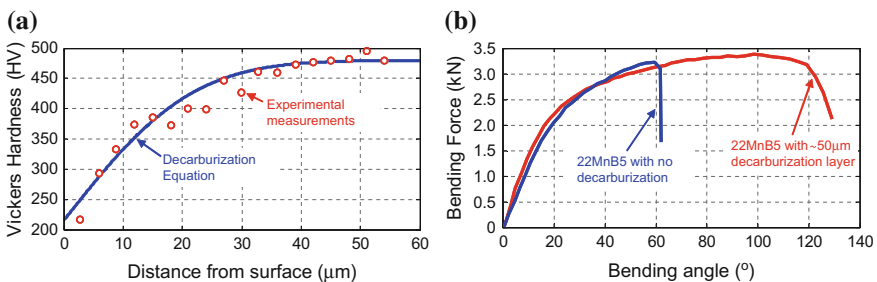


**Fig. 4.13** **a** As the surface layers lose carbon (Decarburization), their hardness is lowered, **b** bendability may be improved by decarburized layers (re-created after [50, 75])

**Table 4.11** Coatings available for hot stamping blanks [1, 3, 8, 21, 74, 80–85]

Coating type (commercial name)	Thickness and chemistry (before/after quenching)	Advantages	Disadvantages
Uncoated (22MnB5, BTR165)	N/A	<ul style="list-style-type: none"> <li>• Cost</li> </ul>	<ul style="list-style-type: none"> <li>• No corrosion protection,</li> <li>• Scale formation,</li> <li>• Decarburization</li> </ul>
AlSi (ArcelorMittal USIBOR, ThyssenKrupp MBW + AS)	AS 150 (150 g/m <sup>2</sup> ) 25 μm AlSi / 40 μm AlSiFe	<ul style="list-style-type: none"> <li>• No scale formation,</li> <li>• Barrier corrosion protection</li> </ul>	<ul style="list-style-type: none"> <li>• No cathodic protection,</li> <li>• Only applicable for direct hot stamping</li> </ul>
	AS 80 (80 g/m <sup>2</sup> ) 13 μm AlSi / 20 μm AlSiFe	<ul style="list-style-type: none"> <li>• Shorter time in furnace</li> </ul>	
Zn (voestalpine phs-ultraform GI)	10 μm Zn / 20 μm ZnFe	<ul style="list-style-type: none"> <li>• Cathodic protection,</li> <li>• Applicable to both direct and indirect hot stamping.</li> </ul>	<ul style="list-style-type: none"> <li>• Surface conditioning may be required,</li> <li>• Risk of LMAC</li> </ul>
ZnNi (ThyssenKrupp GammaProtect)	~10 μm ZnNi / 20–25 μm ZnNiFe	<ul style="list-style-type: none"> <li>• Fast heating possible,</li> <li>• Low friction coefficient (Fig. 4.14a),</li> <li>• Applicable to both direct and indirect processes</li> </ul>	<ul style="list-style-type: none"> <li>• Risk of LMAC.</li> </ul>
Al-Zn (Galvalume)	Not a Standard Coating	<ul style="list-style-type: none"> <li>• Weldable and has good paint adhesion,</li> <li>• Better corrosion protection than GA</li> </ul>	<ul style="list-style-type: none"> <li>• May require a preheating to 550–730 °C,</li> <li>• May result in microcracks.</li> </ul>
Zn-Al-Mg	Not a Standard Coating	<ul style="list-style-type: none"> <li>• Best corrosion protection,</li> <li>• Can be applied as a postprocess coating.</li> </ul>	<ul style="list-style-type: none"> <li>• Risk of LMAC</li> </ul>
(Henkel Bonderite S-FN 7500 PH) Coil Coating	2–3 μm	<ul style="list-style-type: none"> <li>• Fast heating possible,</li> <li>• Weldable without sandblasting</li> </ul>	<ul style="list-style-type: none"> <li>• Coil Application</li> </ul>
Al particles, graphite and wax in inorganic–organic matrix (Nano-X x-tec CO 4020 coil coating)	7 μm Al	<ul style="list-style-type: none"> <li>• Fast heating possible,</li> <li>• Low friction coefficient (Fig. 4.14b)</li> <li>• Easy to apply (Fig. 4.23)</li> <li>• Room Temp. curing</li> </ul>	<ul style="list-style-type: none"> <li>• Has to be removed before painting/welding,</li> <li>• Coil Application</li> </ul>
Al in inorganic matrix (Nano-X Alsi 4001 coil coating)	2–3 μm	<ul style="list-style-type: none"> <li>• Spot weldable,</li> <li>• Suitable for e-coat</li> </ul>	<ul style="list-style-type: none"> <li>• No cathodic protection,</li> <li>• Coil Application,</li> <li>• High temp. curing</li> </ul>

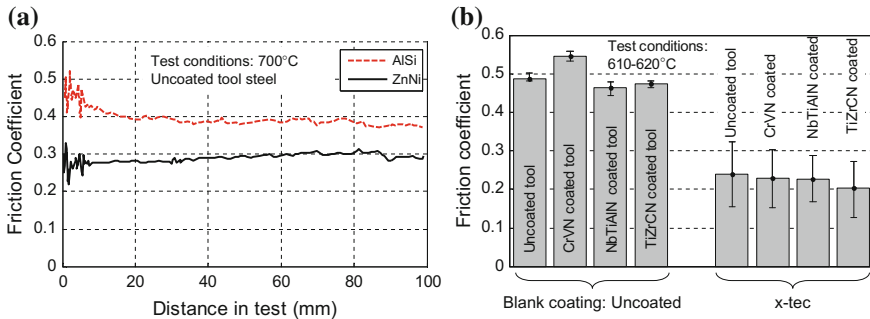


**Fig. 4.14** Friction coefficients of: **a** AISi and ZnNi at 700°C (~1300°F), **b** uncoated and x-tec coated blanks versus several tool coatings tested at 620°C (~1150°F) (re-created after [86, 87])

Blank coatings and the way they are heat treated have great influence on friction during stamping and the final part quality. Friction coefficient of several coatings and uncoated steels are given in Fig. 4.14 [86, 87]. Other important expectations from the coating are:

- (1) weldability,
- (2) compatibility with e-coating and paint baking cycles, and
- (3) corrosion protection [85].

Although uncoated blanks are still used in automotive applications, there are different coatings available on the market, which could be classified under three main types [82]:

- (1) Al-based coatings.
- (2) Zn-based coatings.
- (3) Varnish coatings.

### 4.5.1 Aluminum-Based Coatings

Aluminum-based hot stamping coating was first developed by Usinor, a French steel-maker that was later merged to Arcelor, and then to ArcelorMittal. The first pre-coated steel parts were used in Citroën C5 in 2001 [88–90].

The most common coating used in the recent years is 150 g/m<sup>2</sup> AISi coating. This is equivalent to 25 μm coating thickness before heating. The typical composition is 7–11% Si (nominal 10%) and balance Al. Si is added to form ductile layers in the coating. In the absence of Si, the coating would be very hard but also brittle. Once the pre-coated blank is heated, iron diffusion takes place and forms a 40 μm thick AlSiFe of 5 layers, as shown in Fig. 4.15 [8, 82, 85, 91, 92].

The iron diffusion is a time-dependent process. If the diffusion is not completed (short heating time) the layers would not form as shown in Fig. 4.16a. In a typical process, the blank is kept in the furnace for 5–6 min.s (300–360 s). Layers of coating

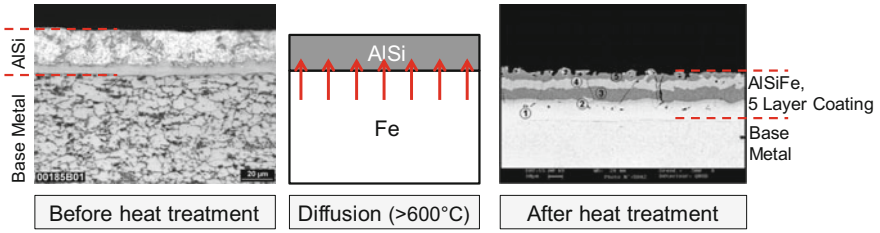


**Fig. 4.15** During heat treatment, Fe diffuses from the base steel to the coating and forms AlSiFe coating (re-created after [95])

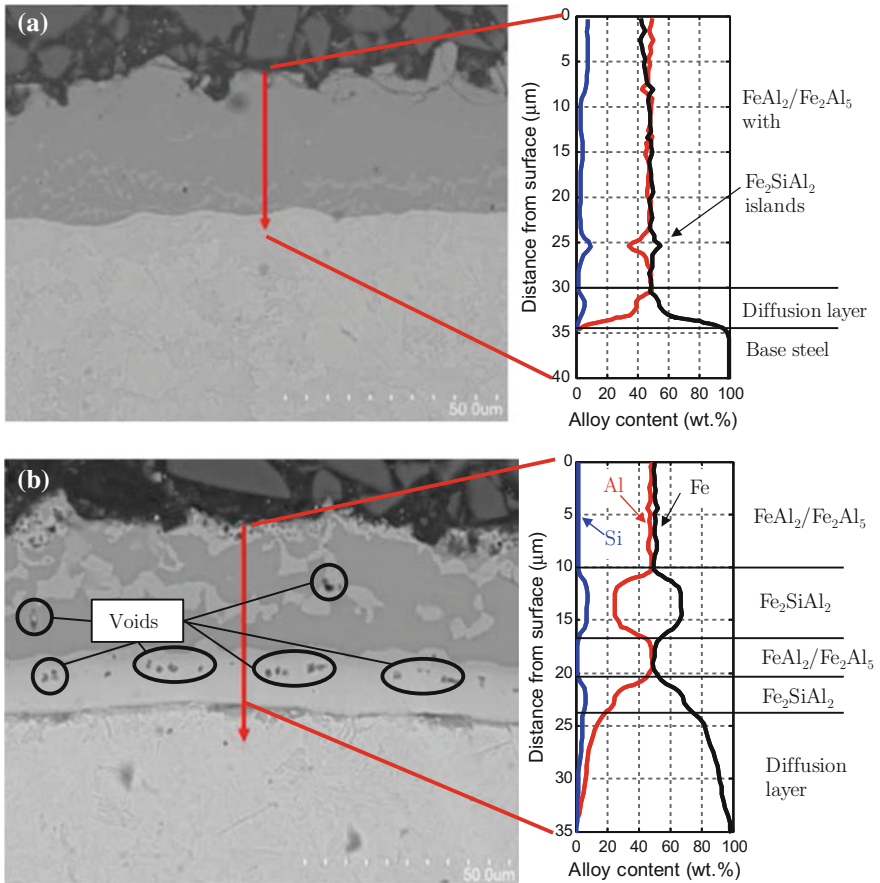


**Fig. 4.16** Coating diffusion after: **a** 2 min, and **b** 6 min, in roller hearth furnace set at 930°C (1700°F) (re-created after [82, 93, 96])

after 6 min in the furnace can be seen in Fig. 4.16b, for a 1.2 mm thick AS150-coated steel [93]. If the blank is heated for longer durations, (1) more voids may occur which increases the porosity of the coating, (2) the total thickness of the coating increases and (3)  $Fe_2Al_5$ ,  $FeAl_2$ , and  $Fe_2SiAl_2$  layers disappear and the coating becomes a single layer of  $\alpha$ -iron with Al and Si in solid solution [8, 82, 94]. The coating diffusion is extremely important for most applications as it will affect:

- (1) weldability of the final part and
- (2) surface properties for painting [91].

AlSi coatings successfully prevent scale formation and decarburization even without an atmosphere controlled furnace. The coating provides barrier corrosion protection. As a disadvantage, these coatings cost more compared to uncoated blanks and require a longer time in the furnace. The total time in furnace is equal to the sum of heating and dwell times, and depends on three variables [21, 95, 97]:

- (1) The initial blank thickness: heating time to ensure austenitization.
- (2) The type of coating: AlSi coating requires a maximum 12 °C/s, as it will melt over this rate.
- (3) The initial coating thickness: dwell time to ensure coating diffusion.

AlSi-coated steels cannot be cold formed (as in indirect hot stamping) as the Fe–Al intermetallic coating is very hard (>600 HV) and brittle during cold deformation. The brittleness of the coating is also critical for the parts produced as their coatings could be damaged in service. Fan and De Cooman showed that the coating could crack easily but the cracks would not propagate to the diffusion layer [82]. For this reason, the thickness of the diffusion layer is critical and has to be controlled. This can be done by controlling the furnace temperature and dwell time [97].

The typical AlSi coating weighs 150 g/m<sup>2</sup>. In 2013, ArcelorMittal developed USIBOR 1500 P AS80 with 80 g/m<sup>2</sup> AlSi coating. There were two rationales behind this development [98]:

- (1) Lower cost, to be more competitive.
- (2) Reduced coating weight would reduce the heating/dwell time in furnace.

Alden [99] has shown that the furnace dwell time could in practice be halved with AS80. Windmann et al. found that the dwell time required to form a single layer coating (which has to be avoided) was 20 min for AS80 and 40 min for AS150 [94]. Both studies prove that the dwell time could be reduced. On the other hand, Fujita [100] has shown that hot-formed steel with AS80 coating had approximately twice the blister width after cyclic corrosion test. Thus, the corrosion resistance is also halved with AS80 coating.

### 4.5.2 Zinc-Based Coatings

AlSi coating provides limited corrosion protection—“barrier protection”—as AlSi coating forms a barrier between the oxidizing environment and the bare steel. How-

ever, most of the car body components are already zinc coated. Thus, a similar level of corrosion protection may also be required in hot-stamped components [101].

Most Zn-based coatings have problems associated with “Liquid Metal Assisted Cracking (LMAC)”. This phenomenon occurs when the coating is in liquid phase (melting point of zinc is around  $420\text{ }^{\circ}\text{C} \sim 790\text{ }^{\circ}\text{F}$  which is much lower than the forming temperatures in hot stamping) and stress is applied to the base metal, which cannot be avoided during metal forming. When both conditions are met, the liquid coating may penetrate into the base metal, causing cracks on the surface, as seen in Fig. 4.19.

To avoid LMAC, Zn-based coated steels were typically indirect hot stamped—where Zn is in solid phase. Indirect hot stamping could be through two different methods [1, 101]:

1. Cold deformation (most of the deformation is done in cold state) followed by hot calibration (very little deformation in hot state).
2. 100% of deformation, cutting, and piercing done at cold forming followed by a “form hardening” (where no deformation is done at hot state).

BMW 7 Series (F01, SOP 2008) was the first car to have Zn-coated hot stamped steel in its body-in-white [102]. Figure 4.17 shows the use of uncoated and Zn-coated boron steels in BMW 5 Series GT, (F07, SOP 2009) [103, 104].

For LMAC to happen there are three prerequisites as shown in Fig. 4.18 [79, 105]:

**(1) Stress level:** during hot stamping stress can be reduced by die design or by improving lubricity (i.e., ZnNi coating has low friction coefficient),

**(2) Presence of liquid metal:** Pure Zn melts at  $420\text{ }^{\circ}\text{C}$  ( $790\text{ }^{\circ}\text{F}$ ), which is far lower than the temperatures in hot stamping process. Therefore, even during heating the blank (i.e., in the furnace) Zn coating on the blank may melt. Thus, liquid

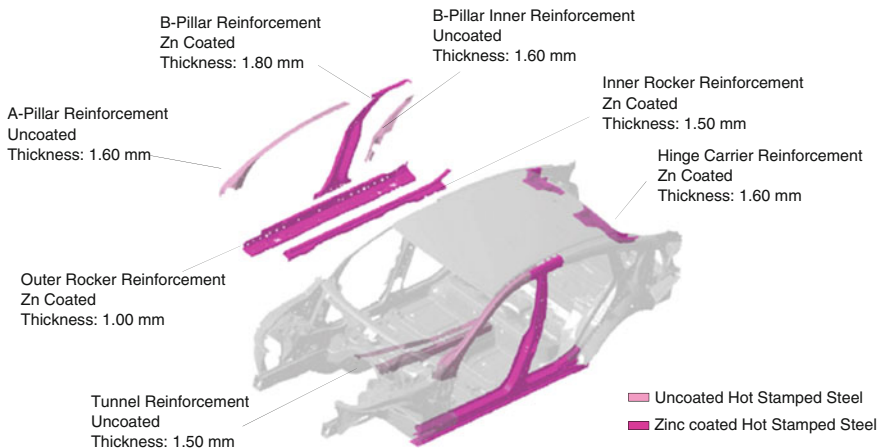


**Fig. 4.17** Usage of hot-stamped steels in BMW 5 Gran Turismo (F07, SOP 2009) (re-created after [104])

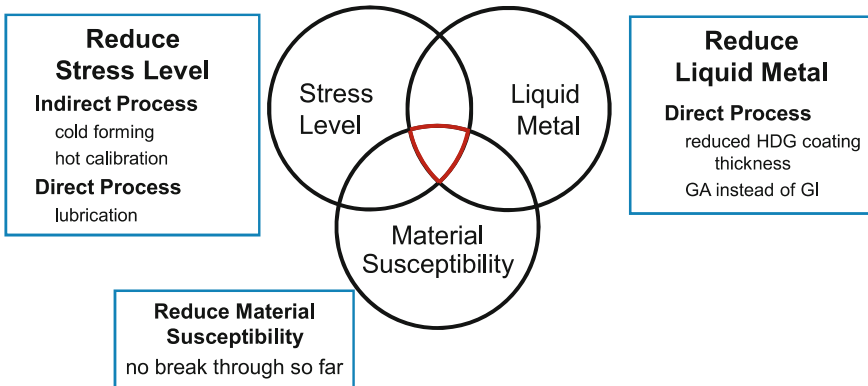


**Fig. 4.18** Factors leading to LMAC (Liquid Metal Assisted Cracking) [21]

metal cannot be avoided if the blank is Zn coated. However, the amount of liquid Zn can be adjusted by the weight of coating (typically given by  $\text{g/m}^2$ ) and the coating technology. Reducing coating weight would sacrifice from cathodic protection and decrease the time required in furnace for coating to diffuse [21]. If the coating is galvanized, iron would diffuse into the coating and increases the melting temperature. Another possibility is to use alloying elements in the coating to increase the melting temperature. One such design was ZnNi coatings [20, 106] (Fig. 4.19).

**(3) Reducing material susceptibility:** covers a number of properties of the steel, including but not limited to (1) chemical composition and carbon equivalence, (2) yield strength/hardness, and (3) residual stresses [105]. In hot stamping grades, no practical method was found to lower material susceptibility [68].

The presence of microcracks could reduce the fatigue life of the components. Kurz has studied the crack depth and fatigue stress. As seen in Fig. 4.20, microcracks up to  $10\ \mu\text{m}$  in the base metal do not affect the fatigue stress. However, if the crack size exceeds  $10\ \mu\text{m}$ , fatigue stress reduces drastically [21].

As the coating weight increases, the time in furnace has to be longer. It was also found that as the depth of microcracks is also affected by the coating weight. To avoid microcracks deeper than  $10\ \mu\text{m}$  in the base metal, GI coating weight is limited to  $70\ \text{g/m}^2$  per side ( $140\ \text{g/m}^2$  total, abbreviated as Z140) [21].

Hot dip galvanized (GI) steels have an iron diffusion during heating, similar to AlSi coating. In GI coatings, 0.2–2.5 wt.% Al is added to form an Al-enriched layer between the steel and Zn coating [82, 108, 109]. After iron diffusion, there has to be three layers, as shown in Fig. 4.21a [110]. The outermost layer is an oxide layer, consisting of aluminum and zinc oxides. This layer is functional during hot stamping as it suppresses evaporation of Zn but has to be removed before welding/painting by sandblasting [82, 98, 109]. Below the oxide layer, Zn-rich  $\Gamma$  phase is found. This layer plays significant role in the corrosion resistance. For adequate cathodic protection, this layer should have at least 70 wt.% Zn. The Fe-rich  $\alpha$  phase determines



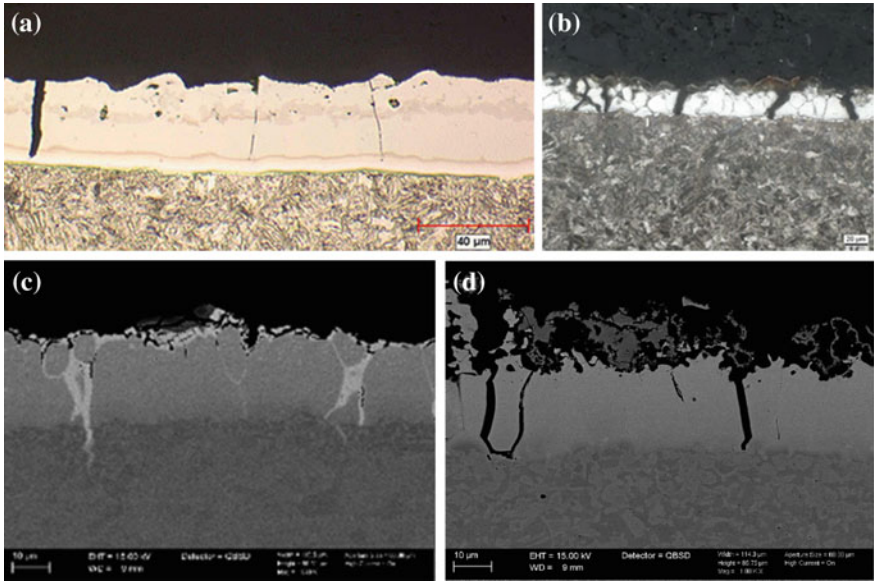


**Fig. 4.19** Coatings after hot stamping: **a** microcracks in AISi coating do not penetrate into steel substrate [8], **b** GI coating melts and Zn may penetrate into base material depending on coating thickness [21]. In **c** GA and **d** ZnAlMg coatings, LMAC problem is reduced but still microcracks may be formed, predominantly not in the base metal [107]

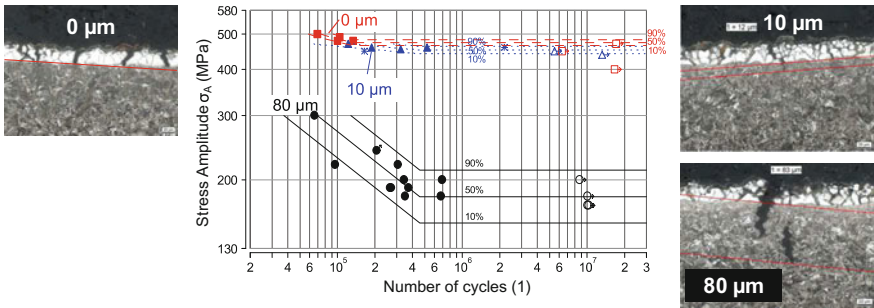


**Fig. 4.20** Effect of microcrack depth in base material on fatigue life of Zn-coated 22MnB5 steel. Micrographs showing the cracks are also shown [21]

the adhesion of coating to the base metal. It should contain at least 10 wt.% Zn, preferably in the range of 17–44 wt.% [82, 109].

Zn coating has relatively narrow process window for hot stamping compared to uncoated and/or AISi-coated blanks. As pure zinc’s boiling point (907 °C ≈ 1665 °F) is very close to the austenitization temperature of 22MnB5 (880 °C ≈ 1615 °F). If furnace dwell time is too short, the coating diffusion would not be completed. If the time is too long, deep microcracks may occur in the base metal [21, 111, 112].



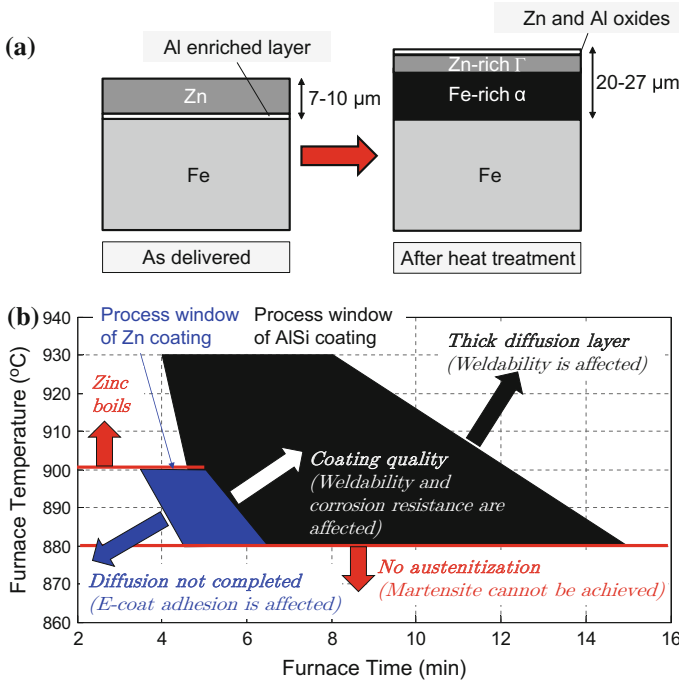


**Fig. 4.21** a Diffusion of Zn (GI) coating (re-created after [82, 110]), b process windows of Zn and AlSi coatings (re-created after [111–114])

To reduce LMAC and/or the need for surface conditioning, alloying elements increasing the melting point of Zn could be added into coating. ZnNi coating was once commercialized by ThyssenKrupp with the name GammaProtect. There were two mass-produced automotive parts using this coating. However, the coating has been discontinued and production was switched to AlSi-coated blanks [20, 111, 115]. Other Zn-alloyed coatings could be ZnFe (Galvannealed coating, abbreviated as GA) and ZnAlMg [92, 108]. Galvannealing (GA) is a process where the galvanized steel is heated to 480–520 °C (~900–970 °F). During this process, iron diffuses into coating and the final coating may have 10–15 wt.% Fe and 85–90 wt.% Zn [116]. GA coatings may be welded and painted without removing the oxide layer [82, 98].

Another recent solution to LMAC is precooling before plastic deformation. Ghanbari [117] found that microcrack formation occurs if forming is done over 782 °C (1440 °F). Kurz et al. [101] developed a precooling stage where the cooling rate is over 50 °C/s (90 °F/s) but the cooling is interrupted before the martensite start temperature, Fig. 4.22a. By this method, forming is still done at austenitic phase [101]. Faderl and Kelsch have shown that if the precooling temperature is lowered, microcrack depth is reduced [118]. At around 550–570 °C (1020–1060 °F), Zn coating is solidified and microcracks are reduced [119, 120]. Typical 22MnB5 could be held at 550 °C (1020 °F) for only 2 s before bainite transformation starts. The newly

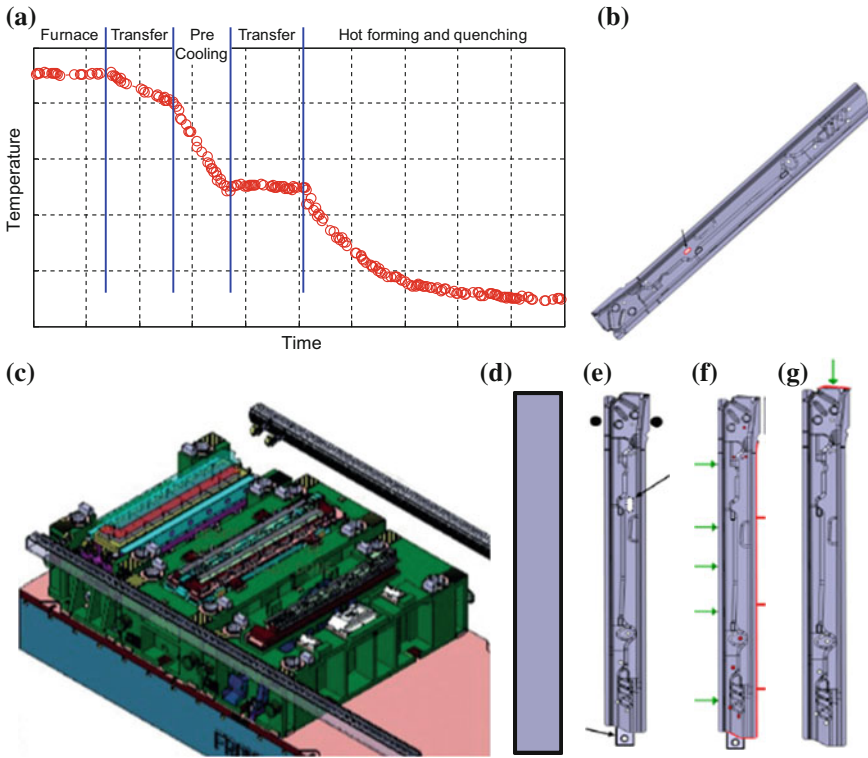


**Fig. 4.22** Multistep hot stamping: **a** the temperature-time profile, including the “precooling” stage, **b** The final part geometry, **c** thermal controlled transfer die set, **d** OP10: Precooling, **e** OP20: Forming, **f** OP30: Cutting/Piercing, and **g** OP40: Cam Trimming (re-created after [20, 101, 121])

designed 20MnB8 alloy can be held at this temperature level for more than 20 s before the transformation [68]. By using precooling system 20MnB8 GA 90/90 (ZF180) can be formed in a multistep operation in a transfer press, as shown in Fig. 4.22b–f.

Currently ArcelorMittal, POSCO, and voestalpine offer Zn GI coatings. ArcelorMittal and voestalpine also offer GA coating. Tata Steel is developing MagiZinc (ZnAlMg) coating for press hardening, but this product is currently not in the market [9, 14, 101, 122]. According to Dormegny [123], 76% of the hot stamping steel in EU27+Turkey is AlSi coated. In these markets, 18% of hot stamping steel is uncoated and only 6% is Zn coated.

### 4.5.3 Varnish Coatings

Another method to avoid scaling and decarburization is to apply varnish coatings. In this method, uncoated blanks are either coil coated or roll coated with the paint-like

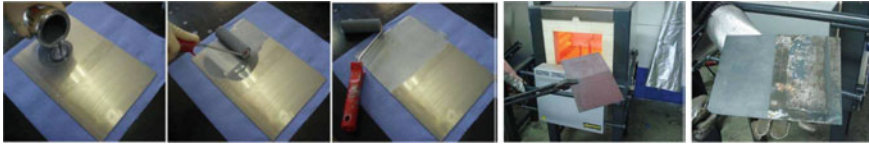


**Fig. 4.23** x-tec coating can be applied simply by a paint roll or spray gun [74]

varnish coatings. The first such application for hot stamping process was developed by Nano-X company in 2005. By then, AlSi coating was already in production. However, in several components of the (then) new Passat, part shapes were extremely complex. A two-step forming process was needed where some deformation would be done by cold forming and more in hot forming, as shown in Fig. 1.15, in Chap. 1 [124, 125].

The first-generation x-tec (see CO 4020 in Table 4.11) had Al particles, graphite and wax in inorganic–organic matrix. This coating should be applied 6–7  $\mu\text{m}$  thick on the uncoated base steel. It can be applied simply by paint rollers (Fig. 4.23) or could be coil coated. cures in room temperature. x-tec coating has lower friction compared to uncoated and AlSi-coated blanks, and was on a par with ZnNi coatings, see Fig. 10.7. This coating had to be removed (by sandblasting) before e-coating and/or welding [74].

Second-generation x-tec, AlSi 4001 as shown in Table 4.11, was developed to be weldable without sandblasting. The coating has high heat absorption and since extra time for diffusion is not required, the total furnace time could be lowered significantly. It can also handle inductive, conductive, and near infrared heating and could be applied as thin as 2–3  $\mu\text{m}$  [74].

In 2015, Henkel has introduced a varnish coating for hot stamping, called Bonderite S-FN 7500 PH. The coating is suitable for fast heating and provides barrier corrosion protection. Although its friction coefficient is not published yet, it helps lubricating the blank. The coating is not required to be removed/sandblasted before e-coating or spot welding [85].

## References

1. H. Karbasian, A.E. Tekkaya, A review on hot stamping. *J. Mater. Process. Technol.* **210**(15), 2103–2118 (2010)
2. T.K. Eller, L. Greve, M.T. Andres, M. Medricky, A. Hatscher, V.T. Meinders, A.H. van den Boogaard, Plasticity and fracture modeling of quench-hardenable boron steel with tailored properties. *J. Mater. Process. Technol.* **214**(6), 1211–1227 (2014)
3. C.W. Lee, W.S. Choi, Y.R. Cho, B.C.D. Cooman, Microstructure evolution of a 55 wt. hardening steel during rapid heating. *Surf. Coat. Technol.* **281**, 35–43 (2015)
4. M. Naderi, Hot stamping of ultra high strength steels. PhD Dissertation, RWTH Aachen, Germany (2007)
5. M. Spittel, T. Spittel, *Steel Symbol/Number: 22MnB5/1.5528* (Springer, Berlin, 2009), pp. 930–935

6. S. Flachstahl, 22MnB5 boron alloyed quenched and tempered steel. Product catalogue (2014)
7. A.K. Steel, ULTRALUME Aluminized Type 1 Press Hardenable Boron Steel. Product catalogue (2016)
8. T. Vietoris, New developments in PHS: materials, coatings, production methods. Presented at AP&T Press Hardening, Next Step Seminar, Novi, MI (2011)
9. ArcelorMittal, Extract from the product catalogue (2015). Accessed 10- June 2015
10. BaoSteel, Automotive advanced high strength steels. Product catalogue (2013)
11. B. Macek, Optimization side crash performance using a hot-stamped B-pillar. Presented at Great Designs in Steel Seminar (2006)
12. K. Hikita, Properties of new TS1800 MPa grade hot stamping steel and components. Presented at Materials in Car Body Engineering 2012, May 10–11, Bad Nauheim, Germany (2012)
13. J.B. Nam, Development of new auto steels and application technology, in *China Automotive Steel Conference, World Steel/CISA* (2013)
14. Posco, Automotive steel data book (2016)
15. SSAB, Docol 1500 Bor. Product catalogue (2013)
16. SSAB, DOCOL PHS 1500. Product catalogue (2015)
17. ThyssenKrupp Steel Europe, *Warmumformung im Automobilbau*. Die Bibliothek der Technik (2012)
18. E. Hilfrich, Trends and potentials of new hotforming steels. Presented at Insight Edition Conference, September 19th, Neckarsulm, Germany (2012)
19. ThyssenKrupp Steel Europe, Mangan-bor-stähle für die warmumformung. Product catalogue (2014)
20. I.M. Gonzalez, O. Straube, Development of zinc coated parts for hotstamping, in *Proceedings of New Developments in Sheet Metal Forming Conference, Stuttgart, Germany* (2016), pp. 265–276
21. T. Kurz, New developments in zinc coated steel for press hardening. Presented at Insight Edition Conference, September 20–21, Gothenburg, Sweden (2011)
22. Y. Bi, Development of advanced automotive materials at WISCO. Presented at the State Key Lab of Rolling and Automation (RAL), Northeastern University (2014)
23. J. Komenda, R. Sandström, M. Tukiainen, Multiple regression analysis of jominy hardenability data for boron treated steels. *Steel Res.* **68**(3), 132–137 (1997)
24. H. Lanzerath, Simulation: enabler for the efficient design of lightweight boron intensive body structures. Presented at Insight Edition Conference, September 20–21, Gothenburg, Sweden (2011)
25. D. Wenk, Global capability: hot stamping. Presented at Global Automotive Lightweight Materials Asia 2014, Shanghai, China, March 26–27 (2014)
26. J. Overrath, F.J. Lenze, S. Sikora, Aktuelle entwicklung der warmumformung im automobilen fahrzeugbau. Bauteile der Zukunft–Methoden und Prozesse, Tagungsband zum 30 (2010)
27. S. Graff, T. Gerber, F.J. Lenze, S. Sikora, About the simulation of microstructure evolution in hot sheet stamping process and the correlation of resulting mechanical properties and crash-performance. In *3rd International Conference on Hot Sheet Metal Forming of High Performance Steel, CHS2, Kassel, Germany* (2011), pp. 323–330
28. H.W. Lee, K.-H. Chung, A new body concept for electric vehicle. Presented at Materials in Car Body Engineering 2012, May 11, Bad Nauheim, Germany (2012)
29. M. Garcia, Remote laser welding. Presented at European Automotive Laser Applications (EALA) 2013, February 19–20, Bad Nauheim, Germany (2013)
30. Y. Zhong, Recently Progress of AHSS in BAOSTEEL, in *Presented at Driving Steel 2016, December 5–7, Kuala Lumpur, Malaysia* (2016)
31. ArcelorMittal Flat Carbon Europe S.A. ArcelorMittal Automotive Product Offer Europe, Android App, V1.0 (2015)
32. H. Matsuoka, K. Fujihara, Mazda cx-5. Presented at EuroCarBody 2011, October 18–20, Bad Nauheim, Germany (2011)
33. Renault Media Services, <http://media.renault.com>
34. SSAB, Data sheet 2115, Docol PHS 1800 (2017)

35. O. Hoffmann, Lightweight steel design in the modern vehicle body. In *Werkstoff-Forum Intelligenter Leichtbau*. Hannover, Germany (2011)
36. voestalpine Steel Division. phs-ultraform@data sheet • 03/2017 (2017)
37. H. Mohrbacher, M. Maikranz-Valentin, Recent progress in the metallurgical development of press hardening steel with improved application properties. Presented at *Materials in Car Body Engineering 2014*, May 13–14, Bad Nauheim, Germany (2014)
38. J. Mura, T. Gerber, S. Sikora, F.-J. Lenze, MBW1900 mit mikrolegierung zur optimierung der technologischen eigenschaften nach dem presshärten, in *Tagungsband zum 7. Erlanger Workshop Warmblechumformung 2012* (2012), pp. 1–10
39. K. Lee, J.-H. Kim, S.-Y. Kwak, Y.-R. Cho, S. Choo, K.-G. Chin, Recent developments of automotive sheet steels. Presented at *Materials in Car Body Engineering 2014*, May 13–14, Bad Nauheim, Germany (2014)
40. SSAB, Let's talk about boron steel. Product catalogue (2015)
41. J. Bian, H. Mohrbacher, Novel alloying design for press hardening steels with better crash performance. Presented at *AIST Symposium*, Vail, Colorado, USA (2013)
42. K. Fahlström, Laser welding of boron steels for light-weight vehicle applications. Licentiate Thesis, Högskolan Väst, Sweden (2015)
43. ThyssenKrupp Steel Europe. Product information for manganese-boron steel for hot forming (2016)
44. C. Wang, M. Maoqiu Wang, J. Shi, W. Hui, H. Dong, Effect of microstructure refinement on the strength and toughness of low alloy martensitic steel. *J. Mater. Sci. Technol.* **23**(05), 659 (2007)
45. D.D. Múnera, A. Pic, D. Abou-Khalil, F. Shmit, F. Pinard, Innovative press hardened steel based laser welded blanks solutions for weight savings and crash safety improvements. *SAE Int. J. Mater. Manf.* **1**, 472–479, 04 (2008)
46. F. D'Aiuto, M.M. Tedesco, Development of new structural components with innovative materials and technological solutions. Presented at *Materials in Car Body Engineering 2015*, April 22–23, Bad Nauheim, Germany (2015)
47. ArcelorMittal Media Services, <http://www.arcelormittal.com/corp/news-and-media>
48. H. Ljungqvist, K. Amundsson, O. Lindblad, The all-new Volvo XC90 car body. Presented at *EuroCarBody 2014*, October 21–23, Bad Nauheim, Germany (2014)
49. voestalpine Media services, <http://www.voestalpine.com/group/en/press>
50. W.S. Choi, B.C. De Cooman, Characterization of the bendability of press-hardened 22MnB5 steel. *Steel Res. Int.* **85**(5), 824–835 (2014)
51. D. Pirronek, L. Kessler, H. Richter, S. Myslowicki, Virtuelle produktentwicklung und crashauslegung von stahl-werkstoffverbundsystemen, in *14. German LS-Dyna Forum, 10–12.10.2016, Bamberg* (2016)
52. H. Ferkel, J.N. Hoffmann, L. Keßler, Resource gentle light weight construction for today's and oncoming mobility, in *The International Conference on New Development in Sheet Metal Forming Technology*, Stuttgart, Germany (2012), pp. 1–16
53. K.H. Hu, G.W. Feng, X.D. Liu, R.D. Han, The effect of heating process on strength and the original austenite grain size of hot forming parts, in *Innovative Research in Hot Stamping Technology*. Advanced Materials Research, vol. 1063 (Trans Tech Publications, Switzerland, 2015), pp. 28–31
54. K. Liu, B. Chi, Y. Zhang, J. Li, Constitutive analysis on thermal-mechanical properties of WHT1300HF high strength steel, in *Proceedings of SAE-China Congress 2015: Selected Papers* (Springer, Singapore, 2016), pp. 309–316
55. BaoSteel, Hot-rolled pickled automotive steel sheets. Product catalogue (2010)
56. T. Fröhlich, Maximum safety and lightweight potential due to use of new high strength steels. Presented at *Outokumpu Experience 2013*, May 22–23, London, UK (2013)
57. P.-O. Santacreu, G. Badinier, J.-B. Moreau, J.-M. Herbelin, Fatigue properties of a new martensitic stainless steel for hot stamped chassis parts, in *SAE Technical Paper* (SAE International, 2015), p. 4

58. J.M. Herbelin, 1000–2000 MPa Martensitic stainless steels for flexible hot forming processes. Presented at Materials in Car Body Engineering 2014, May 13–14, Bad Nauheim, Germany (2014)
59. J.M. Herbelin, MaX: martensitic stainless steel for hot stamping. Product catalogue (2015)
60. G. Badinier, J.-D. Mithieux, P.-O. Santacreu, J.-M. Herbelin, Development of a 1.8 GPa martensitic stainless steel for hot stamping application, in *5th International Conference on Hot Sheet Metal Forming of High Performance Steel, CHS2, Toronto, ON, Canada* (2015), pp. 715–723
61. G. Badinier, J.-B. Moreau, B. Petit, C. Boissy, J.-D. Mithieux, S. Saedlou, J. Paegle, Development of press hardening stainless steels for body-in-white application, in *6th International Conference on Hot Sheet Metal Forming of High Performance Steel, CHS2, Atlanta, GA, USA* (2017), pp. 77–84
62. Q. Han, W. Bi, X. Jin, W. Xu, L. Wang, X. Xiong, J. Wang, P. Belanger, Low temperature hot forming of medium-Mn steel, in *5th International Conference on Hot Sheet Metal Forming of High Performance Steel, CHS2, Toronto, ON, Canada* (2015), pp. 381–389
63. I.A. Mendieta, M.A. Telleria, J.P. Drillet, J.D. Puerta Velasquez, M. Alsmann, J. Clobes, S. Bruschi, A. Ghiotti, European commission. directorate-general for research, and innovation. *Green Press Hardening Steel Grades (GPHS): Final Report*. EUR (Luxembourg. Online). Publications Office (2015)
64. Y. Chang, C.Y. Wang, K.M. Zhao, H. Dong, J.W. Yan, An introduction to medium-Mn steel: metallurgy, mechanical properties and warm stamping process. *Mater. Design* **94**, 424–432 (2016)
65. Y.-K. Lee, J. Han, Current opinion in medium manganese steel. *Mater. Sci. Technol.* **31**(7), 843–856 (2015)
66. H.L. Yi, P.J. Du, B.G. Wang, A new invention of press-hardened steel achieving 1880 MPa tensile strength combined with 16% elongation in hot-stamped, in *5th International Conference on Hot Sheet Metal Forming of High Performance Steel, CHS2, Toronto, ON, Canada* (2015), pp. 725–734
67. R. Rana, C.H. Carson, J.G. Speer, Hot forming response of medium manganese transformation induced plasticity steels, in *5th International Conference on Hot Sheet Metal Forming of High Performance Steel, CHS2, Toronto, ON, Canada* (2015), pp. 391–400,
68. T. Kurz, P. Larour, J. Lackner, T. Steck, G. Jesner, Press-hardening of zinc coated steel - characterization of a new material for a new process. *IOP Conf. Ser.: Mater. Sci. Eng.* **159**(1), 012025 (2016)
69. H.W. Tamlar, J.-U. Becker, R. Wunderlich, K.E. Friedrich, P. Rademacher, TriBond®: hot-rolled clad strip, customized steel composite material from coil. *ThyssenKrupp techforum* **1**, 18–23 (2006)
70. ThyssenKrupp Steel Europe. Multi-layer composite for weight reduction: TriBond. Press Release, 2014
71. ThyssenKrupp Steel Europe. TRIBOND®- high strength and high ductility. Product catalogue (2016)
72. ATZ/MTZ (Wiesbaden), *The Project ThyssenKrupp InCar Plus: Solutions for Automotive Efficiency*. ATZ/MTZ extra (Springer Vieweg, Berlin, 2014)
73. J. Wang, R.W. Hyland Jr, Zinc coated steel with inorganic overlay for hot forming, May 17 2012. US Patent App. 13/317,819
74. G. Frenzer, Nano-x gmbh x-tec®and alsicoat products against scale formation on steel. Presentation at Nano-X (2015)
75. R.G. Baggerly, R.A. Drollinger, Determination of decarburization in steel. *J. Mater. Eng. Perform.* **2**(1), 47–50 (1993)
76. G.E. Totten, *Steel Heat Treatment: Metallurgy and Technologies* (CRC Press, Boca Raton, 2006)
77. S. Kalpakjian, S.R. Schmid, *Manufacturing Engineering and Technology* (Prentice Hall, Englewood Cliffs, 2010)

78. P. Belanger, The future for press hardening in the automotive industry. Presented at AP&T Press Hardening, Next Step Seminar, Novi, MI, October (2011), p. 2011
79. M. Van Genderen, W. Verloop, J. Loiseaux et al., Zinc-coated boron steel, ZnX®: Direct hot forming for automotive applications, in *3rd International Conference on Hot Sheet Metal Forming of High Performance Steel, CHS2, Kassel, Germany* (2011), pp. 145–152
80. K. Lamprecht, G. Deinzer, A. Stich, J. Lechler, T. Stöhr, M. Merklein, Thermo-mechanical properties of tailor welded blanks in hot sheet metal forming processes, in *IDDRG, Graz, Austria* (2010), pp. 37–48
81. J. Banik, Hot forming state-of-the-art and trends. Presented at Insight Edition Conference, September 20–21, Gothenburg, Sweden (2011)
82. D.W. Fan, B.C. De Cooman, State of the knowledge on coating systems for hot stamped parts. *Steel Res. Int.* **83**(5), 412–433 (2012)
83. O. Hoffmann, *Environment oriented light weight design in steel*, in *Ökologischer Leichtbau in Stahl, Hannovermesse Werkstoff-Forum, Hannover, Germany* (2012)
84. Henkel Corporation. BONDERITE®S-FN 7500 PH. Product catalogue (2014)
85. W. Fristad, New coil-applied coating for press-hardening steel. *Proc. Galvatech* **2015**, 892–898 (2015)
86. J. Kondratiuk, P. Kuhn, Tribological investigation on friction and wear behaviour of coatings for hot sheet metal forming. *Wear* **270**(11–12), 839–849 (2011)
87. R. Neugebauer, F. Schieck, S. Polster, A. Mosel, A. Rautenstrauch, J. Schönherr, N. Pierschel, Press hardening – an innovative and challenging technology. *Arch. Civil Mech. Eng.* **12**(2), 113–118 (2012)
88. X. Bano, J.P. Laurent, Heat treated boron steels in the automotive industry, in *39th Mechanical Working and Steel Processing Conference* (1997), pp. 673–677
89. L. Vaissiere, J.P. Laurent, A. Reinhardt, Development of pre-coated boron steel for applications on PSA Peugeot Citroën and Renault bodies in white, in *SAE Technical Paper* (SAE International, 2002), p. 7
90. A. Reinhardt, Development of hot stamped ultra high strength steel parts on the Peugeot 307 and the Citroën C5. Presented at EuroCarBody 2001 - 3rd Global Car Body Benchmarking Conference, Bad Nauheim, Germany (2001)
91. P. Siebert, M. Alsmann, H.J. Watermeier, Influence of different heating technologies on the coating properties of hot-dip aluminized 22MnB5, in *3rd International Conference on Hot Sheet Metal Forming of High Performance Steel, CHS2, Kassel, Germany* (2011), pp. 457–464
92. K.S. Jhaji, Heat transfer modeling of roller hearth and muffle furnace. Master's Thesis, University of Waterloo, Waterloo, ON, Canada (2015)
93. M. Jönsson, The problem with melted Al-Si in the hot stamping furnace, in *Advanced High Strength Steel and Press Hardening: Proceedings of the 3rd International Conference on Advanced High Strength Steel and Press Hardening (ICHSU2016)* (World Scientific, Singapore, 2017), pp. 479–485
94. M. Windmann, A. Röttger, W. Theisen, Formation of intermetallic phases in Al-coated hot-stamped 22MnB5 sheets in terms of coating thickness and Si content. *Surf. Coat. Technol.* **246**, 17–25 (2014)
95. T. Vietoris, Hot stamping with USIBOR1500®. Presented at AP&T Press Hardening, Next Step Seminar, Novi, MI, September 15th (2010)
96. D.W. Fan, H.S. Kim, J.-K. Oh, K.-G. Chin, B.C. De Cooman, Coating degradation in hot press forming. *ISIJ Int.* **50**(4), 561–568 (2010)
97. K. Takagi, E. Nakanishi, T. Yoshida, Aluminum-coated structural member and production method, November 9 2004. US Patent 6,815,087
98. E.J. Watkins, Hot stamping market, materials, coatings, and developments. Presented at Schuler Hot Stamping Workshop, May 14, Dearborn, MI, USA (2013)
99. R. Aldén, Metallurgical investigation in weldability of aluminium silicon coated boron steel with different coating thickness. Bachelor Degree Thesis, KTH Royal Institute of Technology, Stockholm, Sweden (2015)

100. S. Fujita, S.J. Maki, H.I. Yamanaka, M. Kurosak, Corrosion resistance after hot stamping of 22MnB5 steels aluminized with 80g/m<sup>2</sup> c.w. and ZnO coating, in *5th International Conference on Hot Sheet Metal Forming of High Performance Steel, CHS2, Toronto, ON, Canada*, pp. 681–690 (2015)
101. T. Kurz, G. Luckeneder, T. Manzenreiter, H. Schwinghammer, A. Sommer, Zinc coated press-hardening steel - challenges and solutions, in *SAE Technical Paper* (SAE International, 2015), p. 4
102. M. Pfestorf, T. Laumann, Potenziale verzinkter warm umgeformter stähle, in *Tagungsband zum 3. Erlanger Workshop Warmblechumformung* (2008)
103. BMW PressClub Global, <http://www.press.bmwgroup.com>
104. D. Copeland, M. Pfestorf, The body in white of the new BMW 5 Series Gran Turismo. Presented at Great Designs in Steel, Livonia, MI, May 5th (2010)
105. The British Constuctional Steelwork Association, Ltd. Galvanizing structural steelwork: an approach to the management of liquid metal assisted cracking (2005)
106. P. Nash, Y.Y. Pan, The Ni Zn (Nickel Zinc) system. *Journal of Phase Equilibria* **8**(5), 422 (1987)
107. W.C. Verloop, Development of Zn-coated boron steel ZnX at Tata Steel, in *Insight Edition Conference* (2011)
108. C.W. Lee, D.W. Fan, I.R. Sohn, S.-J. Lee, B.C. De Cooman, Liquid-metal-induced embrittlement of Zn-coated hot stamping steel. *Metall. Mater. Trans. A* **43**(13), 5122–5127 (2012)
109. M. Fleischanderl, S. Kolnberger, J. Faderl, G. Landl, A.E. Raab, W. Brandstätter, Method for producing a hardened steel part, US Patent 8,021,497, 20 Sept 2011
110. G. Kim, Quality evluation of Zn coated hot press forming steel. Presented at Materials in Car Body Engineering 2013, May 7–8, Bad Nauheim, Germany (2013)
111. J. Banik, M. Köyer, J. Mura, GammaProtect® - always well protected. Presented at Materials in Car Body Engineering 2013, May 7–8, Bad Nauheim, Germany (2013)
112. C. Allely, J. Petitjean, T. Vietoris, Corrosion resistance of zinc based and aluminized coatings on press-hardened steels for automotive, in *3rd International Conference on Hot Sheet Metal Forming of High Performance Steel, CHS2, Kassel, Germany* (2011), pp. 153–160
113. K. Teshima, Challenges of high-efficiency hot forming processes at Honda. Presented at Forming in Car Body Engineering 2012, September 26–27, Bad Nauheim, Germany (2012)
114. S.P. Bhat, Steel grades and coatings for hot stamping, in *4th PHS Suppliers Forum* (2016)
115. J.N. Belanger, P.J. Hall, J.J. Coryell, J.P. Singh, Automotive body press-hardened steel trends, in *International Symposium on New Developments in Advanced High-Strength Sheet Steels* (2013), pp. 239–250
116. American Society of Metals, *ASM Handbook of "Corrosion"*, vol. 13 (ASM International, 1992)
117. Z. Ghanbari, Zinc coated sheet steel for press hardening. Master's Thesis, Colorado School of Mines, Golden, CO, USA (2014)
118. J. Faderl, R. Kelsch, Galvanized press-hardening steels. Presented at Insight Edition Conference, June 24, Bremen (2015)
119. I. Martin, M. López, P. Raya, A. Sunden, D. Berglund, K. Isaksson, S. Isaksson, Press systems and methods, US Patent 9,492,859, 15 Nov 2016
120. C. Hofer, T. Kurz, H. Clemens, R. Schnitzer, Atom probe study of prior austenite grain boundaries of zinc-coated press hardened steel, in *6th International Conference on Hot Sheet Metal Forming of High Performance Steel, CHS2, Atlanta, GA, USA* (2017), pp. 383–390
121. P. Belanger, New Zn multistep hot stamping innovation. Presented at Great Designs in Steel 2017 (2017)
122. Tata Steel, Magizinc®auto. Product Catalogue (2015)
123. L. Dormegny, Efficient lightweighting with new press hardenable steels. AMS Webinar (2017)
124. S. Sepeur, The company Nano-X GmbH: products for the automotive industry. Presentation at Deutsche Börse, July 10th, Frankfurt, Germany (2006)
125. W. Runge, *Technology Entrepreneurship: A Treatise on Entrepreneurs and Entrepreneurship for and in Technology Ventures*, vol. 2 (KIT Scientific Publishing, 2014)